

Canard phenomenon and localization of oscillations in the Belousov–Zhabotinsky reaction with global feedback

Horacio G. Rotstein^{a)} and Nancy Kopell^{b)}

Department of Mathematics and Center for Biodynamics, Boston University, Boston, Massachusetts 02215

Anatol M. Zhabotinsky^{c)} and Irving R. Epstein^{d)}

Department of Chemistry and Volen Center for Complex Systems, Brandeis University, Waltham, Massachusetts 02454

(Received 26 June 2003; accepted 8 August 2003)

The occurrence of spatial domains of large amplitude oscillation on a background of small amplitude oscillation in a reaction–diffusion system is called localization. We study, analytically and numerically, the mechanism of localization in a model of the Belousov–Zhabotinsky reaction subject to global feedback. This behavior is found to arise from the canard phenomenon, in which a limit cycle suddenly undergoes a significant change in amplitude as a bifurcation parameter, in this case the feedback strength, is varied. In the system studied here, the oscillations arise via a supercritical Hopf bifurcation, but our analysis suggests that the same mechanism is relevant for systems undergoing a subcritical Hopf bifurcation. © 2003 American Institute of Physics.

[DOI: 10.1063/1.1614752]

I. INTRODUCTION

Spatial localized structures are patterns that consist of spatial domains of one type of dynamical behavior embedded in a background of another type, e.g., large amplitude oscillations embedded in a background of steady state or small amplitude oscillations. These patterns offer promise for information storage in physical systems such as cavity solitons in a semiconductor microcavity¹ or in arrays of coupled neurons.² Recent experiments^{3,4} on the photosensitive Ru(bpy)₃-catalyzed Belousov–Zhabotinsky (BZ) reaction in a thin layer of silica gel with photochemical global negative feedback give rise to localized structures consisting of large amplitude oscillations (LAO) on a background of small amplitude oscillations (SAO), demonstrating that such behavior can be generated in relatively simple reaction–diffusion systems. We seek here to gain insight into the origin of this localization phenomenon.

The localized structures that we investigate are special cases of a more general phenomenon, oscillatory clusters, which consist of a small number of (not necessarily connected) spatial domains each oscillating with a common amplitude and phase. We study here the case in which only two different amplitude regimes of oscillations occur, with an amplitude ratio very different from 1. There is a range of intermediate amplitudes that are not observable because they occur for an exponentially small interval of a control parameter.

Our system of interest is the BZ reaction–diffusion system with global feedback. The experimental evidence^{4,5} as well as the analysis in Ref. 6 suggests that the existence of

localized cluster patterns does not depend on diffusion, which plays a secondary role, but rather on the global coupling. Thus, in this paper, as in Refs. 4 and 6, we simplify the situation and study a discrete array of globally coupled oscillators, each displaying identical BZ-type kinetics. Our concept of a cluster reflects the fact that all the oscillators belonging to a single cluster display the same dynamics even if they are not locally connected to each other.

Numerical simulations of Oregonator-type models with global inhibitory coupling^{4,7} qualitatively reproduce the experimentally observed localized clusters as well as other spatiotemporal patterns. Localized clusters are also obtained with the simpler, and easier to analyze, modified FitzHugh–Nagumo (MFHN) model.⁶

Here, we analyze the mechanism of localization using a modified Oregonator model with global inhibitory feedback. We show that localization arises in a manner similar to that found in the FHN-type models studied in Ref. 6, but the globally coupled Oregonator model is more complex, since its global coupling term is nonlinear while the FHN coupling is linear. In studying the mechanism of localization, we use analytical techniques and simulations in a complementary fashion.

As in the FHN-type models analyzed in Ref. 6, the localization phenomenon for Oregonator-type models^{4,7} is intimately connected with the canard phenomenon, the sudden explosion, as a control parameter passes through a value known as the canard critical value, of a limit cycle born at a supercritical Hopf bifurcation. Our results and techniques are valid not only for the specific modified Oregonator model studied in detail here but also for a broader class of generalized Rayleigh–Van der Pol equations.

In Sec. II we briefly review some mathematical aspects of the canard phenomenon and the canard critical value for relaxation oscillators.

^{a)}Electronic mail: horacio@bu.edu

^{b)}Electronic mail: nk@bu.edu

^{c)}Electronic mail: zhabotin@brandeis.edu

^{d)}Electronic mail: epstein@brandeis.edu

In Sec. III we present and analyze the dimensionless modified version of the Oregonator model with global feedback.⁷ This model consists of two equations, which describe the evolution of activator and inhibitor variables. The scaling we have chosen (see Appendix A) allows for a further simplification, valid for small enough values of the inhibitor variable, which reduces the system to a classical Oregonator^{4,8} and which is useful for the calculation of the canard critical value.

In Sec. IV we show that localization can be induced by the global feedback parameter. By assuming the existence of two localized clusters, the system is reduced to two globally coupled oscillators, i.e., to a four-dimensional system. We obtain an expression for the global feedback parameter critical value for each cluster as a function of the parameters of the model and the cluster size, and we present simulations showing that the forcing exerted on each oscillatory cluster by the other does not destroy the localized solution.

In Sec. V we argue that, under appropriate conditions, the mechanism presented here is also valid for models that, when uncoupled, undergo a subcritical Hopf bifurcation rather than the more commonly studied supercritical one. Subcritical bifurcations are often associated with the occurrence of localized structures in a variety of physical systems.^{9–13}

Our conclusions are presented in Sec. VI.

II. THE CANARD PHENOMENON

The globally coupled Oregonator model used in Ref. 7 and the globally coupled FHN type models analyzed in Ref. 6 are particular cases of the general form

$$\begin{aligned} v' &= F(v, w) - \gamma(\langle w \rangle - \bar{w})H(v), \\ w' &= \epsilon G(v, w; \lambda). \end{aligned} \quad (1)$$

In the FHN models, H is constant, while in the Oregonator model, H is an explicit function of v . In Eq. (1), $0 < \epsilon \ll 1$, and the zero level curve $F(v, w) = 0$ is a cubic-like function having one local minimum at (v_m, w_m) and one local maximum at (v_M, w_M) with $v_m < v_M$ and $w_m < w_M$. The function G is a nonincreasing function of w , and the zero level curve $G(v, w; \lambda) = 0$ is an increasing function of v for every λ in a neighborhood of $\lambda = 0$. G is also a decreasing function of λ for all v in a neighborhood of v_m . We further assume that $F = 0$ and $G = 0$ intersect at (\bar{v}, \bar{w}) with $(\bar{v}, \bar{w}) = (v_m, w_m)$ when $\lambda = 0$, and that (\bar{v}, \bar{w}) is an unstable fixed point lying on the central branch of F when $\lambda > 0$. The parameter λ governs the relative position of the w -nullcline with respect to the v -nullcline, as illustrated in Fig. 1. It may be an explicit parameter in the model or implicitly defined as a function of other parameters. The parameter γ controls the strength of the global feedback, and

$$\langle w \rangle = \frac{1}{N} \sum_{k=1}^N w_k. \quad (2)$$

It follows from the assumptions on F and G (referred to as the canard conditions, see Ref. 6 for a more precise description) that, for Eq. (1) with $\gamma = 0$, there exists a Hopf bifurcation point $\lambda_H(\epsilon) \geq 0$. As we vary λ the w -nullcline

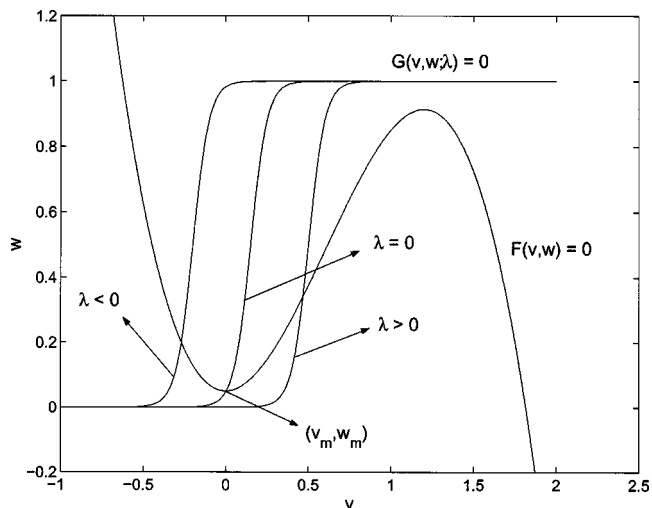


FIG. 1. Schematic representation of the nullclines for a system of type (1) for several values of $\lambda = \bar{v} - v_{\min}$ (the intersection point between nullclines).

shifts until the Hopf bifurcation occurs in a neighborhood of (v_m, w_m) that converges to v_m as $(\epsilon, \lambda) \rightarrow (0, 0)$. There is also a quantity H_c , which depends on the parameters of the model, such that the Hopf bifurcation is supercritical or subcritical according to whether $H_c < 0$ or $H_c > 0$, respectively.^{6,14} For $\lambda < \lambda_H(\epsilon)$, system (1), with the above-made assumptions, has a steady state as its only attractor and is excitable.^{15,16} Both the modified Oregonator model used in Ref. 7 and the FHN type models analyzed in Ref. 6 undergo a supercritical Hopf bifurcation.

In the supercritical case, as λ increases beyond the Hopf bifurcation point, the amplitude of the limit cycle increases slowly for λ not far from $\lambda_H(\epsilon)$. In an exponentially small neighborhood of some critical point, $\lambda_c(\epsilon) > \lambda_H(\epsilon)$, the limit cycle “explodes,” becoming a relaxation oscillator.^{17–19} After that, the amplitude of the limit cycle either increases slowly or remains constant as λ is increased. This behavior is schematically illustrated in Fig. 2, where the amplitude of the limit cycle for a relaxation oscillator is represented by the maximum and minimum values of v and w (v_{\min} , v_{\max} , w_{\min} , and w_{\max}) as a function of λ . In this example λ has been reparametrized to be $\lambda = \bar{v}$.

This rapid change from a “small” amplitude limit cycle to a “large” amplitude limit cycle is known as the canard phenomenon.^{14,19–24} In this case the canard phenomenon has been induced by changes in λ . Here we concentrate on the canard phenomenon near $v = v_m$. Based on techniques and results introduced by Krupa and Szmolyan,^{14,22} we calculated in Ref. 6 an approximation to the value of λ_c as a function of the parameters in a model satisfying the canard assumptions. The key results are summarized in Appendix C and will be used later in our analysis of the modified Oregonator model.

III. A MODIFIED OREGONATOR MODEL WITH GLOBAL INHIBITORY FEEDBACK

A modified version of the Oregonator model was introduced by Zhabotinsky *et al.*²⁵ and extended by Yang *et al.*⁷ to include global feedback. This model simulates the stable

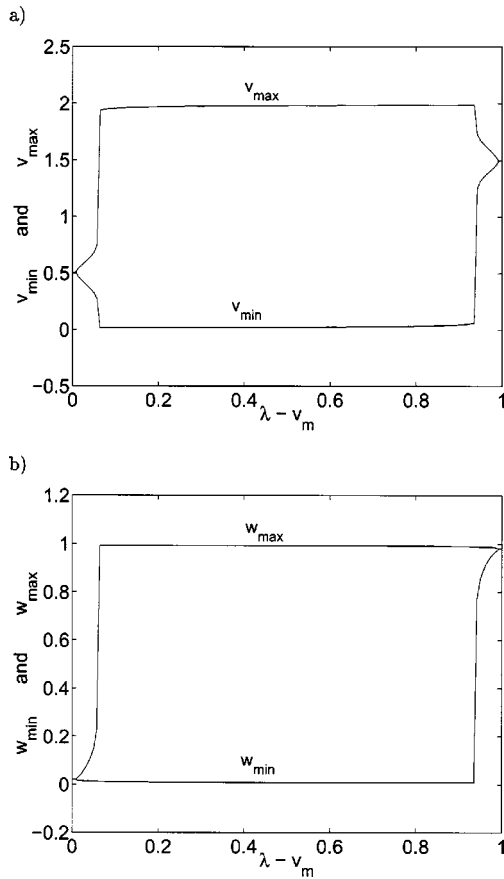


FIG. 2. Schematic representation of the amplitude of the limit cycle as a function of the crossing point between the activator and inhibitor nullclines $\lambda - v_m$ for a single oscillator.

localized solutions whose mechanism we are analyzing and displays the canard phenomenon. In this section we show how this modified Oregonator model can be approximated by the classical Oregonator model, and we calculate the canard critical value for both models.

The dimensional modified Oregonator model used in Ref. 7 and the reduction to dimensionless form of the model analyzed here are presented in Appendix A. The discrete, dimensionless version of the modified Oregonator model with global feedback is given by

$$\begin{aligned} \epsilon_1 dv_k/d\tau &= f(v_k, w_k) - \gamma(\langle w \rangle - \bar{w})\psi(v_k), \\ dw_k/d\tau &= g(v_k, w_k), \end{aligned} \quad (3)$$

for $k=1, \dots, N$, where

$$\begin{aligned} f(v, w) &= \bar{f}(v, w, u) \\ &= -v^2 - \alpha v + \delta u^2 + \eta u(1-w) - \eta v w \\ &\quad - (qw + \beta)\psi(v), \end{aligned} \quad (4)$$

$$u = \frac{2v(\eta w + 2\alpha)}{\eta(1-w) + \sqrt{\eta^2(1-w)^2 + 8\delta v(\eta w + 2\alpha)}}, \quad (5)$$

$$\psi(v) = \frac{v - \mu}{v + \mu}, \quad (6)$$

and

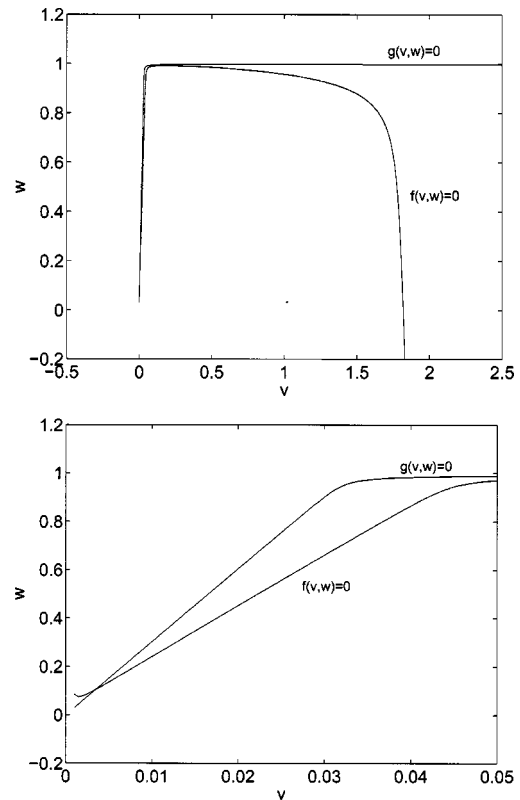


FIG. 3. Nullclines for the dimensionless BZ model. Parameters used in the simulations are listed in Table I. Intersection point between nullclines is $(\bar{v}, \bar{w}) = (0.00295, 0.008153)$.

$$g(v, w) = \bar{g}(v, w, u) = u(1-w) - vw - w. \quad (7)$$

The parameter \bar{w} is the w -coordinate of the intersection point between the nullclines when $\gamma=0$. Note that the intersection point between nullsurfaces does not change with γ .

In the literature, v is usually referred to as the activator variable and w as the inhibitor variable. The activator and inhibitor nullclines are shown in Fig. 3 for the values of the parameters in Table I. System (3) has only one fixed point (\bar{v}, \bar{w}) on the central branch of the activator nullcline which, for the values in Table I, is unstable.

The canard phenomenon occurs near the minimum of the activator nullcline, i.e., where $w \ll 1$. For small w and small δ , $\eta^2(1-w)^2 \gg 8\delta v(\eta w + 2\alpha)$, and Eq. (3) can be simplified by setting $\delta=0$ (see Table I for the actual value of δ). This yields the classical Oregonator model⁸ described in Ap-

TABLE I. Dimensionless parameters used in the simulations.

ϵ_1	0.05
ϵ_2	0.000 004
α	1.826 7
δ	0.000 004
η	0.120 8
q	0.084 54
β	0.000 197
μ	0.000 604
v_m	$\sim 0.001 450$
w_m	$\sim 0.006 424$
λ	0.140 176
κ	0.250 851

pendix B. Equations (3)–(7) with $\gamma=0$ (single oscillator) and v_k , w_k , and u_k replaced by v , w , and u , respectively, become

$$\begin{aligned}\epsilon_1 dv/d\tau &= -v^2 + \alpha v - (qw + \beta)(v - \mu)/(v + \mu), \\ dw/d\tau &= (2\alpha/\eta)v - w.\end{aligned}\quad (8)$$

In an analysis²⁶ of a single classical Oregonator model, the parameter whose change governs the canard explosion was found to be the stoichiometric factor that relates the Br^- production to the oxidized catalyst consumption. In our model this parameter is q .

Variation of q results in displacement of the activator nullcline with respect to the inhibitor nullcline. In order to put Eq. (8) into a more suitable form for the canard analysis we define

$$\lambda = \frac{2\alpha q}{\eta} - \kappa, \quad \kappa = \frac{w_m - \beta}{v_m}, \quad \hat{w} = qw + \beta, \quad (9)$$

and substitute Eq. (9) into Eq. (8) to obtain

$$\begin{aligned}\epsilon_1 dv/d\tau &= -v^2 + \alpha v - \hat{w}(v - \mu)/(v + \mu) \equiv \hat{f}(v, \hat{w}), \\ d\hat{w}/d\tau &= (\lambda + \kappa)v + \beta - \hat{w} \equiv \hat{g}(v, \hat{w}, \lambda).\end{aligned}\quad (10)$$

By this rescaling and change of variables, we have transferred the parameter q or λ , which governs the Hopf bifurcation and the canard explosion, from the activator to the inhibitor equation. It can be shown that $\hat{f}(v_m, w_m) = \hat{g}(v_m, w_m; 0) = 0$, consistent with the formulation in Sec. II. Using Eq. (C3) we can calculate the value of λ_c and from it the value q_c ,

$$q_c = \frac{\eta(\lambda_c + \kappa)}{2\alpha} = \frac{\eta(\Lambda + |F_w|Y)\epsilon_1}{2\alpha} + \frac{\eta(w_m - \beta)}{2\alpha v_m} + \mathcal{O}(\epsilon_1^{3/2}), \quad (11)$$

where the new symbols are defined in Appendix C.

On increasing the value of λ (or equivalently q) in the second equation in Eq. (10), the slope of the inhibitor nullcline increases and the value of v at the crossing point between nullclines decreases, so for $\lambda < \lambda_c$ ($\lambda > \lambda_c$), or equivalently for $q < q_c$ ($q > q_c$), system (10) is in a LAO (SAO) regime. For the parameters listed in Table I we find

$$H_c = -0.475\,441, \quad q_c = 1.683\,964,$$

indicating that the Hopf bifurcation is supercritical, and that since $q < q_c$, system (3) with $\gamma=0$ is in a LAO regime.

IV. LOCALIZED SOLUTIONS INDUCED BY THE GLOBAL FEEDBACK PARAMETER

In this section we analyze the existence of localized solutions for Eqs. (3)–(7). We show that by increasing the value of γ the system can be divided into two clusters, one in a LAO regime and the other in a SAO regime. We use a self-consistent argument, assuming the existence of two clusters and then studying their dynamics and finding conditions under which they exist as a function of the cluster size. We write $\langle w \rangle = \alpha_1 w_1 + \alpha_2 w_2$, where α_1 and α_2 are the fractions

of oscillators in each cluster ($\alpha_1 + \alpha_2 = 1$). System (3) can then be reduced to a four-dimensional system describing the dynamics of two globally coupled oscillators

$$\begin{aligned}\epsilon_1 dv_k/d\tau &= f(v_k, w_k) - \gamma\alpha_k(w_k - \bar{w})\psi(v_k) \\ &\quad - \gamma\alpha_j(w_j - \bar{w})\psi(v_k), \\ dw_k/d\tau &= g(v_k, w_k),\end{aligned}\quad (12)$$

for $j, k = 1, 2, j \neq k$, where f , g , and ψ are given by Eqs. (4), (6), and (7), respectively. Each cluster can be seen as a forced oscillator. Its autonomous part (obtained by setting $\alpha_j = 0$) is analogous to a system of equations for bulk oscillations and describes the phenomenon of self-inhibition of each cluster. The nonautonomous term of each set of cluster equations, the last term in the first equation of Eq. (12), is the force exerted on each cluster by the other. Note that in contrast to Ref. 6, the global feedback term in Eq. (12) is nonlinear.

We continue to use Eq. (8), adding the global feedback term to get

$$\begin{aligned}\epsilon_1 dv_k/d\tau &= -v_k^2 + \alpha v_k - [qw_k + \beta + \gamma\alpha_k(w_k \\ &\quad - \bar{w})]\psi(v_k) - \gamma\alpha_j(w_j - \bar{w})\psi(v_k), \\ dw_k/d\tau &= (2\alpha/\eta)v_k - w_k,\end{aligned}\quad (13)$$

for $j, k = 1, 2, j \neq k$.

We first study Eq. (13) with $\alpha_j = 0$, i.e., we disregard the forcing term.

For a given value of q and a fixed value of α_k , changes in γ produce changes in the position of the activator nullcline relative to the inhibitor nullcline, which in turn changes the canard critical value q_c . At the same time, the minimum of the activator nullcline moves. The formulation in Sec. II requires w_m to be independent of γ . In order to achieve that condition, we follow the ideas of Sec. III and define

$$\begin{aligned}\lambda_k(\gamma) &= \frac{2\alpha(q + \alpha_k\gamma)}{\eta} - \kappa_k(\gamma), \\ \kappa_k(\gamma) &= \frac{w_m - \beta + \alpha_k\gamma\bar{w}}{v_m},\end{aligned}$$

and

$$\hat{w}_k = (q + \alpha_k\gamma)w_k + \beta - \alpha_k\gamma\bar{w}. \quad (14)$$

Substituting Eq. (14) into Eq. (13), we obtain

$$\begin{aligned}\epsilon_1 dv_k/d\tau &= -v_k^2 + \alpha v_k - \hat{w}_k\psi(v_k) \\ &\quad - \alpha_j\gamma(\hat{w}_j - \beta + \gamma\bar{w})/(q + \alpha_k\gamma)\psi(v_k), \\ d\hat{w}_k/d\tau &= [\lambda_k(\gamma) + \kappa_k(\gamma)]v_k - \hat{w}_k + \beta - \alpha_k\gamma\bar{w},\end{aligned}\quad (15)$$

for $j, k = 1, 2, j \neq k$.

In the autonomous part of Eq. (15), this change of variables transfers the global feedback term from the activator to the inhibitor equations, while maintaining the linearity of the inhibitor nullcline.

For the autonomous part of Eq. (15) ($\alpha_j = 0$) the values of λ_c and q_c can be obtained from Eq. (11) using Eq. (C3) and Eq. (14). The values of Λ and Y , and hence λ_c and q_c will depend on α_k and γ . We call these values $\Lambda_k(\gamma)$, $Y_k(\gamma)$, $\lambda_{k,c}(\gamma)$ and $q_{k,c}(\gamma)$, respectively. We find that

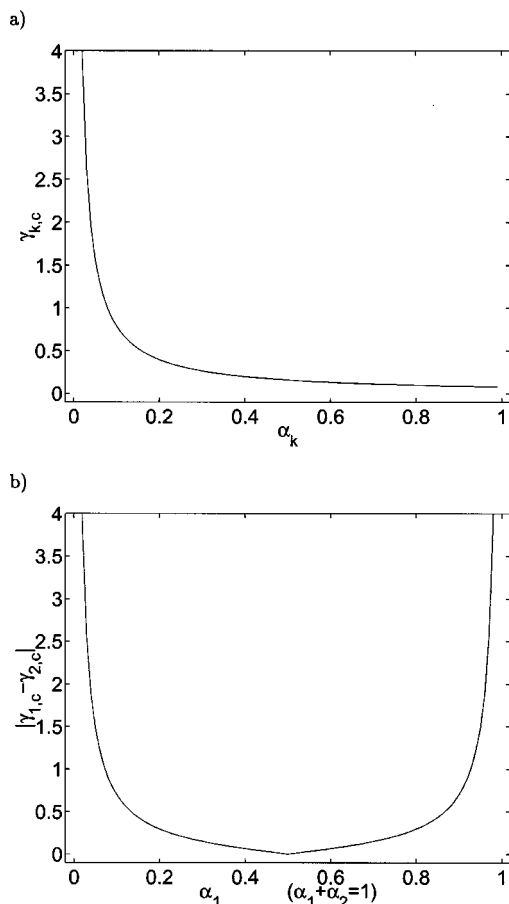


FIG. 4. (a) Dependence of the critical global feedback parameter value $\gamma_{k,c}$ on cluster size. (b) Dependence of the interval of global feedback parameter values for which a localized solution exists on cluster size.

$$q_{k,c}(\gamma) = \frac{\eta[\lambda_{k,c}(\gamma) + \kappa_k(\gamma)]}{2\alpha} - \alpha_k \gamma$$

$$= \frac{\eta(\Lambda_k(\gamma) + |F_w|Y_k(\gamma))\epsilon_1}{2\alpha} + \frac{\eta(w_m - \beta)}{2\alpha v_m} - \alpha_k \gamma + \mathcal{O}(\epsilon^{3/2}). \quad (16)$$

When q and α_k are fixed, $q_{k,c}(\gamma)$ decreases almost linearly with γ . Numerical calculations show that for some value $\gamma_{k,c}$ of γ , $q_{k,c}$ equals q_c for the single (uncoupled) oscillator, i.e., the canard transition is induced by γ (even though q is kept constant) for a possibly different value of γ in each cluster. At this point, the system switches from a LAO to a SAO regime. The dependence of $\gamma_{k,c}$ on α_k is shown in Fig. 4(a). In Fig. 4(b), we see the dependence of $|\gamma_{1,c} - \gamma_{2,c}|$, i.e., the width of the parameter interval in which localization occurs, on the division of oscillators between clusters. In the absence of forcing exerted by the remaining oscillators, as the difference in cluster sizes decreases (α_1 increases from 0 to 0.5) the domain of localized behavior shrinks. Similar results are found in FHN-type models.⁶

In order to test whether or not the forcing exerted by each oscillator on the others destroys the localization, we performed numerical simulations using the modified Oregonator model (A1)–(A5). In Fig. 5 we show the amplitude of the solutions as a function of γ for several values of α_1 and

α_2 . The localization phenomenon persists, and the interval $\gamma_{c,2} - \gamma_{c,1}$ increases with $\alpha_1 - \alpha_2$. The localized solutions found in our simulations are numerically stable in an array of 100 oscillators for γ in a subinterval of $(\gamma_{c,1}, \gamma_{c,2})$. For values of γ outside these intervals (in a neighborhood of the canard implosion for each oscillator) the localized solutions are not stable, and irregular patterns are created. This phenomenon is connected with irregular mixed mode oscillations produced near the canard implosion. The study of this behavior is beyond the scope of this paper.

From our analysis and simulations in these discrete models, we suggest that the mechanism of localization in continuous reaction–diffusion systems is based on the canard process, i.e., as the strength of the global feedback increases, there is a range in which the canard phenomenon is induced in one cluster but not in the other. We thus have a portion of the system in a LAO regime and the other portion in a SAO regime, which constitutes a localized solution.

The localized clusters found in Refs. 3 and 4 consist of one cluster in a SAO regime, which occupies most of the reactor, and two phase-locked clusters in a LAO regime. Equation (13) can be used to study such a three-cluster system by replacing the nonautonomous term $\alpha_j w_j$ (forcing exerted on each oscillator by the others) with $\sum_{j \neq k} \alpha_j w_j$. The analysis of the autonomous part, obtained by setting $\alpha_j = 0$ for $j \neq k$, is identical to the analysis for a two-cluster system, and the results obtained earlier in this section, including Eq. (16), still apply. Following the same reasoning as above, three-cluster localized solutions may be obtained for $\alpha_1 > \alpha_2 \geq \alpha_3$, where cluster 1 is the one in the SAO regime.

V. CHANGE OF HOPF BIFURCATION CRITICALITY INDUCED BY THE GLOBAL FEEDBACK PARAMETER

When the oscillators are uncoupled, oscillations in the modified Oregonator model studied here and the FHN-type models analyzed in Ref. 6 arise via a supercritical Hopf bifurcation; i.e., a single stable limit cycle is created as a parameter passes through a critical value. This monostability is an important assumption for the mechanism of localization we have proposed. Oregonator models that undergo a subcritical Hopf bifurcation are common in the chemical literature.^{8,15} In those models, a stable fixed point and a stable limit cycle in a LAO regime coexist in an interval of values of the bifurcation parameter with an unstable limit cycle in a SAO regime. Here we show that for an oscillator that undergoes a subcritical Hopf bifurcation when uncoupled, a supercritical Hopf bifurcation is induced by adding global coupling to its autonomous part for values of the global feedback parameter $\gamma < \gamma_{k,c}$. Thus, the mechanism of localization studied in this manuscript is applicable to the case of subcritical Hopf bifurcation as well.

Consider the autonomous part of system (1) with homogeneous (v -independent) global inhibitory feedback. We call α_k the fraction of oscillators in the corresponding cluster,

$$v'_k = F(v_k, w_k) - \gamma \alpha_k w_k + \alpha_k \gamma \bar{w},$$

$$w'_k = \epsilon G(v_k, w_k; \lambda), \quad (17)$$

for $k = 1, 2, \dots, N$.

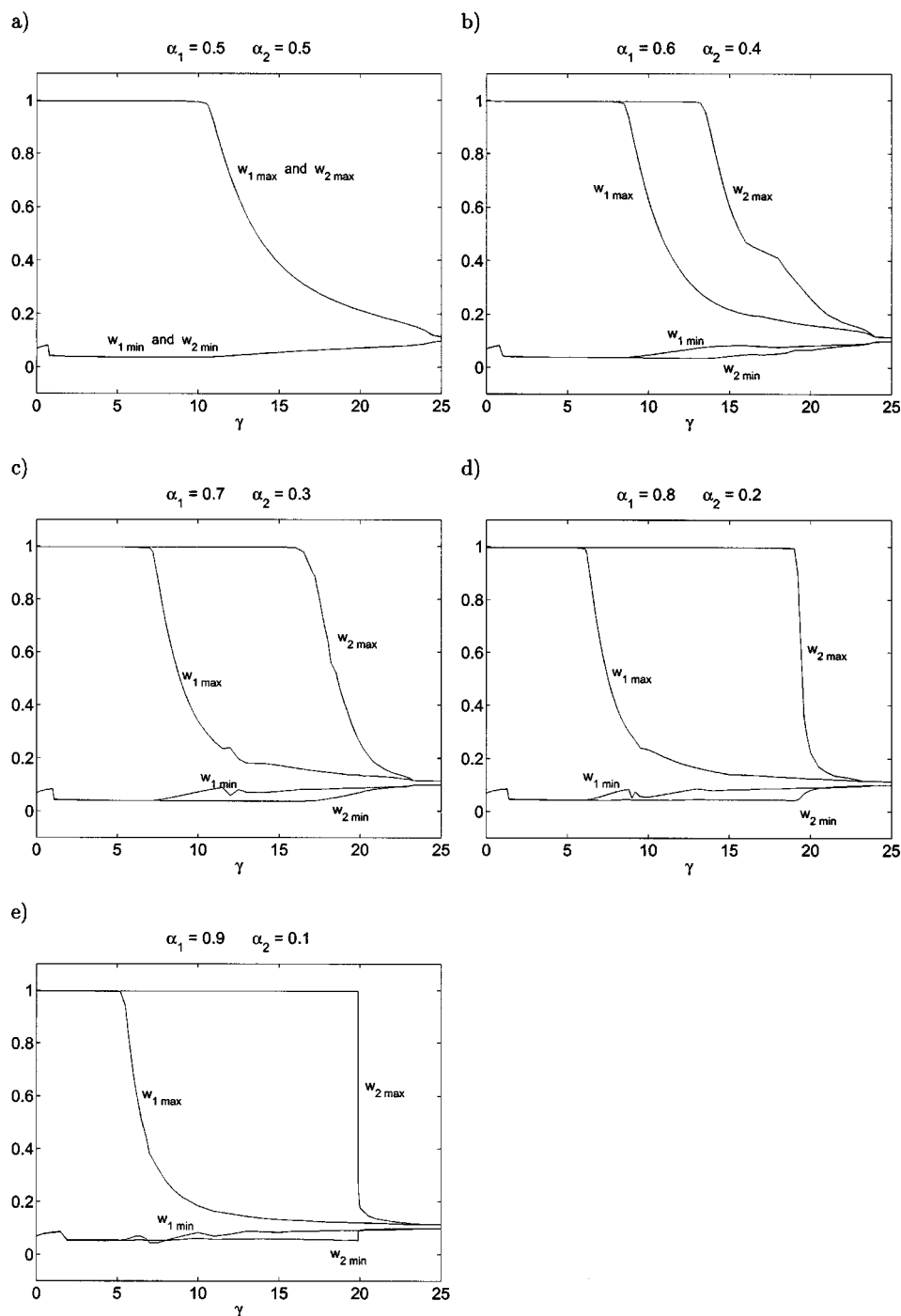


FIG. 5. Amplitude of the limit cycle for two globally coupled BZ oscillators as a function of the global feedback parameter γ . Parameters are listed in Table I. (a) $\alpha_1=0.5$, (b) $\alpha_1=0.6$, (c) $\alpha_1=0.7$, (d) $\alpha_1=0.8$, (e) $\alpha_1=0.9$.

We will use the notation $\bar{\lambda}(\epsilon)=\lambda/\epsilon$. In Ref. 6 the following expression for γ_c as a function of λ_c for different values of α_k was derived,

$$\gamma_c = (\bar{\lambda} - \bar{\lambda}_c(0))/Y,$$

where Y is given by Eq. (C4).

The values of the Hopf bifurcation point λ_H and H_c for system (17) are given by Eq. (C1) with $|F_w|$ replaced by $|F_w| + \gamma$:

$$\bar{\lambda}_H(\sqrt{\epsilon}, \gamma) = -\frac{G_w}{2(G_v)^{1/2}(|F_w| + \gamma)^{1/2}} + \mathcal{O}(\epsilon^{1/2}), \quad (18)$$

$$H_c(\gamma) = \frac{2}{(|F_w| + \gamma)^{1/2}(G_v)^{1/2}(F_{vv})^2} [G_v F_{vv} F_{vw} + |F_w| G_v F_{vvv} - |F_w| G_{vv} F_{vv} - G_w (F_{vv})^2] - \frac{4\gamma F_{vv} |G_\lambda|}{G_v^{3/2}(|F_w| + \gamma)^{1/2}} Y = \frac{|F_w|^{1/2}}{(|F_w| + \gamma)^{1/2}} H_c(0) - \frac{4\gamma F_{vv} |G_\lambda|}{G_v^{3/2}(|F_w| + \gamma)^{1/2}} Y, \quad (19)$$

calculated at (v_m, w_m) .

From Eq. (18) we see that as γ increases, λ_H decreases and $\lim_{\gamma \rightarrow \infty} \lambda_H = \mathcal{O}(\epsilon^{1/2}) > 0$. We also see that the first term on the right-hand side in Eq. (19) decreases as γ increases, and the second term is positive for $\gamma > 0$. Thus if the Hopf bifurcation for the uncoupled system is subcritical, i.e., $H_c(0) > 0$, then there exists a value of γ given by

$$\gamma_0 = \frac{G_v^{3/2} |F_w|^{1/2} H_c(0)}{4 F_{vv} |G_\lambda| Y}, \quad (20)$$

for which $H_c(\gamma) < 0$ for $\gamma > \gamma_0$, i.e., the Hopf bifurcation for bulk oscillations is supercritical.

VI. DISCUSSION

In this paper we have analyzed the phenomenon of localization in Oregonator-type models with global inhibitory feedback. To make detailed analysis tractable, we have replaced the continuous reaction–diffusion system by a discrete model consisting of N coupled oscillators. Experimental and theoretical evidence^{4–6} suggests that the existence of localized patterns depends mostly on global coupling while diffusion plays a secondary role, probably increasing the likelihood that the members of a cluster are contiguous. Numerical simulations were performed using the modified Oregonator model (3)–(7), while analysis was done on a simplified version of the classical Oregonator type (8). The latter was shown to be a good approximation to the former in a neighborhood of the minimum of the activator nullcline, where the relevant behavior occurs. By treating the oscillators in a cluster as a single oscillator, we are able to reduce the problem to that of a small number of globally coupled clusters. Changing variables so as to transfer the global feedback from the activator nullcline to the inhibitor nullcline enabled us to effectively convert a nonlinear feedback to a linear one. We were then able to utilize several of the results obtained⁶ from analysis of the simpler FitzHugh–Nagumo-type models, where the global feedback is linear. The key element of our mechanism is that for bulk oscillations, i.e., the oscillations of a single cluster, the canard phenomenon can be induced by increasing the global feedback parameter γ beyond a critical value γ_c , where the behavior changes suddenly from LAO to SAO. For clusters of different sizes, this transition occurs at different values of γ , so that there is an interval of γ in which the clusters are in different regimes, i.e., the structure is localized. Numerical simulations confirm that this phenomenon is robust to the introduction of forcing interactions among the oscillators, occurs for the experimentally relevant situation of three clusters, and is stable in arrays of up to 100 oscillators, thus encouraging us in our extrapolation of this behavior to continuous reaction–diffusion systems.

Since the forcing exerted by a SAO cluster has a relatively small effect on LAO clusters, the existence of M -cluster localized solutions, $M \geq 4$, with one cluster in a SAO regime and $M - 1$ in a LAO regime is consistent with the results obtained from our analysis of (only) self-inhibition. However, stable localized solutions with more than three clusters have not been found, either experimentally or numerically, for reasons that are still not understood.

To better understand structures in which there are two large amplitude phase-locked clusters,^{4,7} we did simulations that reveal a relationship between cluster size and cluster phase. We found (data not shown) that when a system has two clusters in a LAO regime (not localized), the magnitude of the phase difference decreases as the difference between the relative fraction of oscillators in each cluster increases. When the system is divided into two equal clusters, the clusters are in antiphase. Since, in a localized system, the cluster in the SAO regime exerts only a small forcing on the clusters in the LAO regime, we argue that this relation is qualitatively valid in the large amplitude clusters in localized solutions with more than one cluster in a LAO regime. Numerical simulations of the full globally coupled system suggest, however, that *stable* localized three-clusters must satisfy $\alpha_1 > \alpha_2 + \alpha_3$, a result consistent with experimental observations. A rigorous analysis of this stability is beyond the scope of this paper.

There exists a great deal of experimental evidence for the existence of small amplitude oscillations, transition from steady state to large amplitude relaxation oscillations (with and without hysteresis) and transition from small amplitude oscillations to large amplitude relaxation oscillations in homogeneous (stirred) chemical systems.^{27–36} Other types of sudden transitions to LAO regimes have been reported.^{37–39} Theoretical studies have been performed on canard explosions in a model of iodate oxidation of sulfite and ferrocyanide,⁴⁰ in models of autocatalytic chemical reactions,^{41–44} in the Brusselator model,²³ in the Oregonator model,^{26,37} and in the Edblom–Orbán–Epstein model.⁴⁵

Previous studies of canard explosions in reaction–diffusion systems have been much more limited. The effect of diffusion-induced instabilities near a canard has been studied⁴⁶ in a modified version of the Oregonator.²⁵ By analyzing in detail the applicability of the canard phenomenon in spatially distributed systems, we provide here a theoretical framework for understanding the localization phenomena found recently in experiments involving global feedback. Our proposed mechanism explains the inverse relation between amplitude regime and cluster size and sheds light on the role of self-inhibition in the phenomenon of localization.

ACKNOWLEDGMENTS

The authors thank Tasso Kaper and Kresimir Josic for helpful suggestions on the mathematical treatment of the canard phenomenon, Milos Dolnik for useful comments on the BZ reaction, and the canard group at Boston University for the collective learning experience on the mathematics of canards. This work was partially supported by the Burroughs Wellcome Fund (H.G.R.), NSF Grant No. CHE-9988463 (I.R.E. and A.M.Z.), and NSF Grant No. DMS-0211505 (N.K.).

APPENDIX A: A MODIFIED OREGONATOR MODEL FOR THE BZ REACTION

1. Dimensional formulation

The modified Oregonator model proposed in Ref. 25 and used in the simulations in Ref. 7 is given by

$$\begin{aligned} V' &= F(V, W, U), \\ W' &= G(V, W, U), \\ U' &= H(V, W, U), \end{aligned} \quad (\text{A1})$$

where

$$\begin{aligned} F(V, W, U) &= \frac{-k_2 V + k_3 A}{k_2 V + k_3 A} \left[\frac{Q k_7 k_8 B W}{k_8 + k_{-7} h_0 (C - W)} \right. \\ &\quad \left. + k_9 B \right] - 2k_4 V^2 + k_5 h_0 A V - k_{-5} U^2, \quad (\text{A2}) \end{aligned}$$

$$\begin{aligned} G(V, W, U) &= k_6 U (C - W) - k_{-6} V W \\ &\quad - \frac{k_7 k_8 B W}{k_8 + k_{-7} h_0 (C - W)}, \quad (\text{A3}) \end{aligned}$$

and

$$H(V, W, U) = 2k_5 h_0 A V - 2k_{-5} U^2 - k_6 U (C - W) + k_{-6} V W. \quad (\text{A4})$$

A quasi-steady state approximation for U , equivalent to setting $H(V, W, U) = 0$ in Eq. (A4), can be made.⁷ System (A1) then becomes two-dimensional, with

$$U = \frac{-k_6 (C - W) + \sqrt{[k_6 (C - W)]^2 + 8k_{-5} (2k_5 h_0 A V + k_{-6} V W)}}{4k_{-5}}. \quad (\text{A5})$$

The values of the parameters used in our simulations were taken from Ref. 7: $Q = 0.7$, $h = 0.55$, $k_2 = 2 \times 10^6$, $k_3 = 2$, $k_4 = 3000$, $k_5 = 33$, $k_6 = 4 \times 10^6$, $k_7 = 0.92$, $k_8 = 2.5 \times 10^{-4}$, $k_9 = 3 \times 10^{-6}$, $k_{-5} = 4.2 \times 10^6$, $k_{-6} = 3 \times 10^2$, $k_{-7} = 1$, $A = 0.5$, $B = 0.27$, $C = 2 \times 10^{-3}$, $V_{ss} = 0.003383$, and $W_{ss} = 0.102345$ where (V_{ss}, W_{ss}) is the intersection point between the nullclines.

2. Dimensionless formulation

In order to put system (A1) into dimensionless form, we define the following variables and parameters:²⁵

$$v = \frac{k_{-6}}{k_7 B} V, \quad w = \frac{1}{C} W, \quad u = \frac{k_6}{k_7 B} U, \quad (\text{A6})$$

$$x = \left(\frac{k_7 B}{D_W} \right)^{1/2} x, \quad \tau = k_7 B t, \quad (\text{A7})$$

$$\epsilon_1 = \frac{k_{-6}}{2k_4}, \quad \epsilon_2 = \frac{k_{-6}^2}{2k_4 k_6}, \quad \beta = \frac{k_9 k_{-6}^2}{2k_7^2 k_4 B}, \quad (\text{A8})$$

$$q = \frac{Q k_{-6}^2 C}{2k_4 k_7 B}, \quad \eta = \frac{k_{-6}^2 C}{2k_4 k_7 B}, \quad \alpha = \frac{k_5 h_0 A k_{-6}}{2k_4 k_7 B}, \quad (\text{A9})$$

$$\delta = \frac{k_{-5} k_{-6}^2}{2k_6^2 k_4}, \quad \mu = \frac{k_3 k_6 A}{k_2 k_7 B}. \quad (\text{A10})$$

Substituting Eqs. (A6)–(A10) into Eqs. (A1)–(A4), we get

$$\begin{aligned} \epsilon_1 dv/d\tau &= \bar{f}(v, w, u), \\ dw/d\tau &= \bar{g}(v, w, u), \\ \epsilon_2 du/d\tau &= \bar{h}(v, w, u), \end{aligned} \quad (\text{A11})$$

where

$$\begin{aligned} \bar{f}(v, w, u) &= -v^2 - \alpha v + \delta u^2 + \eta u(1 - w) \\ &\quad - \eta v w - (q w + \beta) \psi(v), \end{aligned} \quad (\text{A12})$$

$$\psi(v) = \frac{v - \mu}{v + \mu}, \quad (\text{A13})$$

$$\bar{g}(v, w, u) = u(1 - w) - v w - w, \quad (\text{A14})$$

$$\bar{h}(v, w, u) = 2\alpha v - 2\delta u^2 - \eta u(1 - w) + \eta v w. \quad (\text{A15})$$

We let \bar{w} be the w -coordinate of the intersection point of the three nullsurfaces when $\gamma = 0$. Adding a global feedback term to the first equation in Eq. (A11),⁷ we get

$$\begin{aligned} \epsilon_1 dv/d\tau &= \bar{f}(v, w, u) - \gamma(\langle w \rangle - \bar{w})\psi(v), \\ dw/d\tau &= \bar{g}(v, w, u), \\ \epsilon_2 du/d\tau &= \bar{h}(v, w, u). \end{aligned} \quad (\text{A16})$$

By making the quasi-steady state approximation with respect to u , we get Eq. (3); Eq. (5) is obtained by setting $\bar{h} = 0$ in Eq. (A15), calculating u_k and multiplying and dividing the result by the conjugate of the numerator.

APPENDIX B: AN OREGONATOR MODEL FOR THE BZ REACTION

A nondimensional version of the Oregonator model proposed by Tyson^{8,47} is given by

$$\begin{aligned} \bar{\epsilon}_1 x' &= \bar{\alpha} y - x y + x(1 - x), \\ \bar{\epsilon}_2 y' &= -\bar{\alpha} y - x y + \bar{q} z, \\ z' &= x - z, \end{aligned} \quad (\text{B1})$$

where $\bar{\alpha}$, \bar{q} , $\bar{\epsilon}_1$, and $\bar{\epsilon}_2$ are positive constants and $\bar{\epsilon}_2 \ll \bar{\epsilon}_1$. Making the quasi-steady state assumption on the second equation in Eq. (B1), we get

$$\begin{aligned} \bar{\epsilon}_1 x' &= -x^2 + x - \bar{q} z(x - \bar{\alpha})/(x + \bar{\alpha}), \\ z' &= x - z. \end{aligned} \quad (\text{B2})$$

APPENDIX C: HOPF BIFURCATION AND CANARD CRITICAL VALUE

For system (1) the Hopf bifurcation point is given by

$$\lambda_H(\sqrt{\epsilon}) = -\frac{G_w}{2(G_v)^{1/2}|F_w|^{1/2}}\epsilon + \mathcal{O}(\epsilon^{3/2}). \quad (\text{C1})$$

The parameter H_c , which determines whether the bifurcation is super- or subcritical, is given by

$$H_c = \frac{2}{|F_w|^{1/2}(G_v)^{1/2}(F_{vv})^2} [G_v F_{vv} F_{vw} + |F_w| G_v F_{vvv} - |F_w| G_{vv} F_{vv} - G_w (F_{vv})^2], \quad (\text{C2})$$

and the canard critical value is given by

$$\lambda_c = (\Lambda + |F_w|Y)\epsilon + \mathcal{O}(\epsilon^{3/2}), \quad (\text{C3})$$

where

$$Y = \frac{G_v}{2F_{vv}|G_\lambda|} \left(\frac{G_v}{F_{vv}} \right)_v, \quad (\text{C4})$$

$$\Lambda = -\frac{G_v}{2F_{vv}^3|G_\lambda|} (G_v F_{vv} F_{vv} + G_w F_{vv}^2),$$

and where all functions are calculated at $v=v_m$ and $w=w_m$. Note that if $(v_m, w_m) \neq (0,0)$ expression (C3) is still valid, provided the conditions defining a canard point are satisfied at (v_m, w_m) .

¹S. Barland, J. R. Tredicce, M. Brambilla *et al.*, *Nature* (London) **419**, 699 (2002).

²D. Golomb and J. Rinzel, *Physica D* **72**, 259 (1994).

³V. K. Vanag, L. Yang, M. Dolnik, A. M. Zhabotinsky, and I. R. Epstein, *Nature* (London) **406**, 389 (2000).

⁴V. K. Vanag, A. M. Zhabotinsky, and I. R. Epstein, *J. Phys. Chem. A* **104**, 11566 (2000).

⁵V. K. Vanag, A. M. Zhabotinsky, and I. R. Epstein, *Phys. Rev. Lett.* **86**, 552 (2001).

⁶H. G. Rotstein, N. Kopell, A. Zhabotinsky, and I. R. Epstein, *SIAM J. Appl. Math.* (to be published). (A preprint may be found at <http://math.bu.edu/people/horacio/publications>)

⁷L. Yang, M. Dolnik, A. M. Zhabotinsky, and I. R. Epstein, *Phys. Rev. E* **62**, 6414 (2000).

⁸R. J. Field and M. Burger, *Oscillations and Traveling Waves in Chemical Systems* (Wiley, New York, 1985).

⁹O. Thual and S. Fauve, *J. Phys.* **49**, 1829 (1998).

¹⁰O. Jensen, V. O. Pannbacker, E. Mosekilde, G. Dewel, and P. Borckmans, *Phys. Rev. E* **50**, 736 (1994).

¹¹H. Sakaguchi and H. R. Brande, *Europhys. Lett.* **38**, 341 (1997).

¹²B. Ermentrout, X. F. Chen, and Z. Chen, *Physica D* **108**, 147 (1997).

¹³M. Tlidi, P. Mandel, and M. Haelterman, *Phys. Rev. E* **56**, 6524 (1997).

¹⁴M. Krupa and P. Szmolyan, *J. Diff. Eqns.* **174**, 312 (2001).

¹⁵J. D. Murray, *Mathematical Biology* (Springer, Berlin, 1989).

¹⁶S. H. Strogatz, *Nonlinear Dynamics and Chaos* (Addison-Wesley, Reading, MA, 1994).

¹⁷E. F. Mishchenko and N. Kh. Rozov, *Differential Equations with Small Parameters and Relaxation Oscillations* (Plenum, New York, 1980).

¹⁸J. Grasman *Asymptotic Methods for Relaxation Oscillations and Applications* (Springer, New York, 1986).

¹⁹W. Eckhaus, *Lect. Notes Math.* **985**, 449 (1983).

²⁰F. Dumortier and R. Roussarie, *Mem. Am. Math. Soc.* **121**, 577 (1996).

²¹E. Benoit, J. L. Callot, F. Diener, and M. Diener, *Chasse au Canard* (IRMA, Strasbourg, 1980).

²²M. Krupa and P. Szmolyan, *SIAM J. Math. Anal.* **33**, 286 (2001).

²³S. M. Baer and T. Erneux, *SIAM (Soc. Ind. Appl. Math.) J. Appl. Math.* **46**, 721 (1986).

²⁴F. Dumortier, in *Bifurcations and Periodic Orbits of Vector Fields*, edited by D. Schlomiuk (Kluwer Academic, Dordrecht, 1993), p. 19.

²⁵A. M. Zhabotinsky, F. Buchholtz, A. B. Kiyatkin, and I. R. Epstein, *J. Phys. Chem.* **97**, 7578 (1993).

²⁶M. Krupa, W. F. Langford, and J. P. Voroney (unpublished).

²⁷J. Maselko, *Chem. Phys.* **67**, 17 (1982).

²⁸J. Maselko, *Chem. Phys.* **78**, 381 (1983).

²⁹R. A. Schmidt, K. R. Graziani, and J. L. Hudson, *J. Chem. Phys.* **67**, 3040 (1977).

³⁰K. R. Graziani, J. L. Hudson, and R. A. Schmitz, *Chem. Eng. J.* **12**, 9 (1976).

³¹J. L. Hudson, M. Hart, and D. J. Marinko, *J. Chem. Phys.* **71**, 1601 (1979).

³²M. Alamgir and I. R. Epstein, *J. Am. Chem. Soc.* **105**, 2500 (1983).

³³M. Orbán and I. R. Epstein, *J. Phys. Chem.* **87**, 3212 (1983).

³⁴A. Nagy and L. Treindl, *J. Phys. Chem.* **93**, 2807 (1989).

³⁵E. C. Edblom, Y. Luo, M. Orbán, K. Kustin, and I. R. Epstein, *J. Phys. Chem.* **93**, 2722 (1989).

³⁶F. Berthier, J. P. Diard, and S. Nagues, *J. Electroanal. Chem.* **436**, 35 (1997).

³⁷M. Brøns and K. Bar-Eli, *J. Phys. Chem.* **95**, 8706 (1991).

³⁸J. Boissonade and P. De Kepper, *J. Phys. Chem.* **84**, 501 (1980).

³⁹K. Bar-Eli and M. J. Brøns, *J. Phys. Chem.* **94**, 7170 (1990).

⁴⁰V. Gáspár and K. J. Showalter, *J. Phys. Chem.* **94**, 4973 (1990).

⁴¹S. K. Scott and A. S. Tomlin, *Philos. Trans. R. Soc. London, Ser. A* **332**, 51 (1990).

⁴²A. Milik and P. Szmolyan, in *Multiple Time-Scale Dynamical Systems*, IMA Volume, edited by C. K. R. T. Jones and A. Khibnik (Springer, New York, 2000), p. 122.

⁴³V. Petrov, S. K. Scott, and K. Showalter, *J. Chem. Phys.* **97**, 6191 (1992).

⁴⁴M. Brøns and J. Sturis, *Phys. Rev. E* **64**, 026209 (2001).

⁴⁵E. C. Edblom, M. Orbán, and I. R. Epstein, *J. Am. Chem. Soc.* **108**, 2826 (1986).

⁴⁶F. Buchholtz, M. Dolnik, and I. R. Epstein, *J. Phys. Chem.* **99**, 15093 (1995).

⁴⁷J. J. Tyson, *Ann. N.Y. Acad. Sci.* **316**, 279 (1979).